

Serveur Académique Lausannois SERVAL serval.unil.ch

Preprint Author Manuscript

Faculty of Biology and Medicine Publication

This paper does not include the final publisher revision, proof-corrections or journal pagination.

Published in final edited form as:

Title: Separation of small metabolites and lipids in spectra from biopsies by diffusion-weighted HR-MAS NMR: a feasibility study.

Authors: Diserens G., Vermathen M., Precht C., Broskey N.T., Boesch C., Amati F., Dufour J.F., Vermathen P.

Journal: [Analyst](#)

Year: 2014

DOI: [10.1039/c4an01663g](https://doi.org/10.1039/c4an01663g)

In the absence of a copyright statement, users should assume that standard copyright protection applies, unless the article contains an explicit statement to the contrary. In case of doubt, contact the journal publisher to verify the copyright status of an article.

Separation of Small Metabolites and Lipids in Spectra from Biopsies by Diffusion-weighted HR-MAS NMR. A Feasibility Study.

Gaëlle Diserens¹, Martina Vermathen², Christina Stahl³, Nicholas T. Broskey⁴, Chris Boesch¹, Francesca Amati^{1,4}, Jean-François Dufour⁵ and Peter Vermathen¹

¹Depts Clinical Research and Radiology, University of Bern, Bern, Switzerland, ²Dept. of Chemistry & Biochemistry, University of Bern, Bern, Switzerland, ³Dept. of Clinical Veterinary Medicine, Clinical Radiology, Vetsuisse-Faculty, University of Bern, Bern, Switzerland, ⁴Dept. of Physiology, University of Lausanne, Lausanne, Switzerland, ⁵Hepatology, Dept. Clinical Research and University Clinic for Visceral Surgery and Medicine, Inselspital, University of Bern, Bern, Switzerland

1. Introduction

It has been shown that high resolution magic angle spinning (HR-MAS) NMR allows to metabolically characterize biopsies from different tissues like brain, prostate, liver, or muscle (1). Fast spinning around an axis inclined at the magic angle (54.7°) averages orientation dependent effects, thereby reducing the spectral linewidth.

However, HR-MAS spectra from tissues of most organs show strong contributions from broad lipid signals. Although these may convey important information themselves, they are overlapping metabolite regions. This could hamper metabolite estimation and may lead to misinterpretation. Metabolite quantification and metabonomic analysis would therefore benefit from a separation of lipid resonances from those of small metabolites.

Spectral fitting may be applied for separating lipids from small metabolites (2). However, solely fitting the lipid contribution in spectra that contain also small metabolites is prone to artificial inclusion of metabolite contributions into the lipid fit. Fitting simultaneously small metabolites and lipids has many advantages, but it also introduces bias as to which metabolites to include and also on the included metabolites themselves, which is avoided in metabonomic analysis.

The Carr-Purcell-Meiboom-Gill (CPMG) sequence is commonly used as a T₂-filter to reduce broad components and therefore also fat contributions from spectra, taking advantage of the short T₂ relaxation times of lipids(3). However, long echo times would be required to eliminate most of the lipids(4), with consequently (A) reduced signal to noise also for small metabolites, (B) a T₂ dependency of peak intensities impeding metabolite quantification, (C) heating of the sample, (D) J-evolution of spins, and (E) losing all information on lipids.

Besides shorter T₂, lipids differ also from small metabolites in terms of much slower diffusion. Fast diffusing small metabolites may therefore be separated from slow diffusing lipids by NMR diffusion measurements. It has previously been shown that subtracting a strongly diffusion weighted (DW) spectrum from a low DW spectrum can lead to a strong reduction or even elimination of spectral contributions from lipids. This was applied in high resolution liquid state NMR measurements of proteins (5), carbohydrates (6), as well as in rat (7) and human blood plasma (8), and in in-vivo measurements of the brain(9).

Moreover, an almost complete separation of small molecules and lipids may be obtained by a combination of both physical differences, i.e. combining diffusion gradient editing and T₂-filter (10). The two effects have been combined in oil-water samples (11) for separate measurements of individual T₂ attenuations of the two components, and conversely in vegetables for improved separated determination of diffusion constants (12). In liver biopsies, the two effects have been combined for distinguishing lipid and low molecular weight resonances for both improved relaxation and diffusion constant estimations, as this

can provide information of metabolite changes inside the tissue (4). Liu et al. showed the possibility to separate the high molecular weight molecules by diffusion editing, the low molecular weight molecules by relaxation editing and applied a combined editing method (combined diffusion and T2-filter sequence) in human blood plasma for better lipoprotein analysis(8).

However, to the best of our knowledge, diffusion gradient editing alone or its combination with a T2-filter has not yet been applied in HR-MAS spectra of biopsies for obtaining lipid-free small metabolite spectra.

The aim of our study was therefore to investigate different diffusion editing techniques in order to employ diffusion differences for separating lipid from small metabolite contributions in the spectra of various tissues for unbiased metabolomic analysis. Thus NMR-diffusion measurements applying different gradient strengths were performed on biopsies of human muscle. Spectra obtained at strong DW solely consisting of lipid signals were subtracted from those obtained at low DW including both, small metabolites and lipids. In addition, the study aimed at simultaneously utilizing diffusion and T2 differences (12) between small metabolites and lipids for an efficient separation. Therefore additional measurements were performed on biopsies from different organs and animals combining both effects.

In order to probe the impact of this editing method, it was applied in a reproducibility study of muscle spectra including chemometric analyses. The metabolite variability of two specimen of the same muscle was investigated before and after removing the lipid peaks. Secondary aim was to determine to what extent the metabolite profile of a single muscle specimen can be considered representative for the tissue.

2. Material and Methods

2.1 Biopsies

In order to test the lipid removal method under very different conditions, biopsies from different organs and animals were analyzed. The diffusion editing technique was tested and improved in human and pork muscle, sheep brain, and human liver biopsies. The method was then applied in a reproducibility study on human muscle. For all measurements on human and animal biopsies ethical approval was obtained.

2.1.1 Human Muscle Biopsy - Reproducibility study

The human muscle biopsies included in this study were measured as part of an on-going clinical trial involving healthy adults (13). Skeletal muscle specimens were obtained from the *vastus lateralis* by the Bergstrom technique under local anaesthesia (2% lidocaine) as described previously (14). After retrieval, specimens were immediately trimmed from fat with a magnification lens (10x), flash frozen in liquid nitrogen and stored at -80 degrees until analyzed. As each needle biopsy pass allows the collection of multiple specimens with possible distances of a few millimetres, 8 pairs of biopsies (4.1 ± 2.4 mg) were used for the reproducibility analyses (labelled "same needle biopsies").

2.1.2 Sheep brain biopsy

Five sheep brain biopsies ($10.5\text{mg} \pm 1.8\text{mg}$) were obtained by stereotactic-guided brain biopsy collection from thalamus and brainstem. Out of these five biopsies, three were from a slaughtered healthy sheep collected two hours after death, and two were from two living

and healthy sheep. 70% ethanol was used for aseptic skin preparation. All these biopsies were simultaneously analyzed for an on-going sheep brain clinical study.

2.1.3 Human liver

Two human liver biopsies were obtained from an ongoing hepatic steatosis study (approx. 5mg). The two subjects showed 80% and 50% steatosis in histology. The liver biopsy was performed transcutaneously with a 17G Menghini needle after sonography localization and local anesthesia with lidocaine. The tissue was kept unfixed and frozen in TissueTek.

2.1.4 Pork muscle

Fresh tissue samples of three pork muscles (approx. 8mg) from commercial meat were obtained to optimize measurement parameters.

2.2 ^1H High Resolution Magic Angle Spinning (HR-MAS) NMR

^1H HR-MAS NMR experiments were performed on a Bruker Avance II spectrometer (Bruker Karlsruhe, Germany) operating at a resonance frequency of 500.13 MHz using a 4 mm HR MAS dual inverse ^1H / ^{13}C probe with a Magic Angle gradient. The measurements were performed between 277 and 282 Kelvin according to the tissue type. In a preceding experiment the temperature control was calibrated under same MAS conditions using a sample of 4% MeOH in MeOD- d_4 . Bruker TOPSPIN software (version 2.1, patch level 5) was used to acquire and process the NMR data. For all measurements the tissue was washed and placed together with D_2O -based phosphate buffered saline (PBS, pH=7, 50mM) into the zirconium MAS rotor using a 12 μl insert.

2.2.1 CPMG (T2-filter)

CPMG measurements with presaturation of the water signal were performed on all samples ("*cpmgpr1d*" from the Bruker pulse-program library). The measurements were performed at an echo time (TE) of 76.8 ms (192 loops, rotor-synchronized interpulse delay of 0.4 ms) and a recycle delay of 4s, with a magic angle spinning speed of 5kHz. Each CPMG spectrum was acquired applying 512 transients, a spectral width of 7002.8 Hz and a data size of 64K points. These measurements were used as reference for spectral quality and were employed for the reproducibility study with and without subtraction of the lipid contribution.

Additional CPMG measurements were performed on pork biopsies for parameter optimization, modifying TE, the number of loops and the interpulse delay time for each loop. The four following combinations were used: (1) TE of 76.8ms with 192 loops of 0.4ms; (2) TE of 152ms with 380 loops of 0.4ms; (3) TE of 152ms with 38 loops of 4ms; (4) TE of 760ms with 380 individual loops of 2ms each.

2.2.2 2D-Diffusion

2.2.2.1 2D-diffusion for investigating diffusion properties and for "internal" lipid removal

Diffusion measurements were first performed using a modified 2D stimulated echo experiment with bipolar gradient pulses and longitudinal eddy current delay ("*ledbpgp2s2d*" from the Bruker pulse-program library), at a magic angle spinning speed of 8 kHz. The higher spinning speed was selected, because preceding measurements demonstrated a higher stability of the 2D-diffusion data. Diffusion times Δ were 50ms and 200ms and the gradient pulse length δ was 6ms. Linear ramps of 64 different values of sinusoidal gradient pulses, varying from 0.6 to 32 G/cm, were used. 16 scans were acquired at every gradient-strength with a recycle delay of 2s.

The 2D-diffusion measurements were processed conventionally to create and analyze pseudo-2D DOSY spectra, using Bruker Dynamics Center 2.0.8. In addition the individual spectra of the 64 different DW were investigated. Spectra at stronger gradients, which exhibited purely lipid signals, were added, yielding a pure lipid spectrum with good SNR. Depending on the number of added spectra, the weightings of different lipid components vary, if the diffusion constants are different. It turned out that for $\Delta = 50\text{ms}$ ideally the last 20 spectra could be added to yield a pure lipid spectrum [see results section 3.2.2]. This summed spectrum was then subtracted from the summed spectrum at low gradient strength (the first 20 individual spectra of the series were selected for best SNR).

2.2.2.2 2D-diffusion for lipid removal from CPMG spectra for reproducibility study

The 2D-diffusion sequence and the described add/subtract procedure were applied in spectra from human muscle biopsies. For same needle biopsy samples, the lipid spectrum from 2D-Diffusion was obtained on only one biopsy of each pair and then subtracted from the CPMG measurements of both biopsies after individual scaling of each lipid peak.

2.2.3 1D-Diffusion

Additional measurements were performed at a spinning speed of 5 kHz on pork muscle, sheep brain and human liver biopsies combining 1D and 2D diffusion sequences with a CPMG train as a T2 filter. Each 1D-diffusion spectrum was acquired applying 1024 acquisitions, a spectral width of 6009.6 Hz and a data size of 32K points. 1D-measurements were performed twice, once with very low DW (0.1 G/cm) and once with strong weighting (20 G/cm or 32 G/cm), yielding a mixed small metabolite/lipid spectrum and a pure lipid spectrum, respectively, both with very good SNR. The high-diffusion-weighted spectrum was scaled to the lipid peak at 1.3ppm of the low-diffusion-weighted spectrum, and was subtracted from the low-weighted spectrum, in order to get a lipid-free spectrum.

2.2.4 Post-processing

For all spectra, the co-added free induction decays (FIDs) were exponentially weighted with a line broadening factor of 1.0 Hz, Fourier-transformed, phased and frequency calibrated to creatine at 3.03 ppm to obtain the ^1H NMR spectra.

2.3 Muscle data analysis

Using literature references (15-21) and our own additional 2D correlation spectroscopy ($^1\text{H}^1\text{H}$ -TOCSY) measurements, an overall of 18 metabolites and 11 lipid resonances were assigned.

For chemometric analysis of the muscle biopsies for the reproducibility study, a total of 63 buckets (between 0.95 and 8.62 ppm) were selected, with a variable size according to the peak width (see supplementary material, figure S1). Spectral regions comprising only noise and pure lipid regions were excluded from all analyses to facilitate a comparison of the small metabolite content from the original and lipid-subtracted CPMG spectra. In addition, some spectra were contaminated by lidocaine, the anaesthetic agent. Five spectral regions with potential contributions from lidocaine resonances (peaks at 1.37, 2.2, 3.37, 4.45, 7.21, 7.26 ppm) were also excluded from the analysis. The buckets were normalized by probabilistic quotient normalization (PQN) (22) and scaled with Pareto scaling, which keeps the influence of noise low, while decreasing contributions from intense peaks and increasing the weight of intermediate peaks (23). MatLab (R2011b, The MathsWorks Inc.) was used for statistical analysis.

The whole muscle analysis (bucketing, normalization, scaling and statistical analysis) was first done on the pure CPMG spectra, and then repeated with the lipid-subtracted CPMG spectra [see 2.2.2.2], to evaluate the influence of the lipid removal on the reproducibility metabonomic study.

3. Results and Discussion

The lipid removal edited method was first applied with 2D-diffusion measurements in human muscle biopsies to investigate and account for the impact of differences in diffusion times. The lipid removal was then improved by combining a 1D diffusion sequence with a CPMG train as T2 filter and tested in several organs. Finally, the applicability and potential value of the lipid removal procedure was tested in a small reproducibility study on same-needle biopsies.

3.1 2D-Diffusion of human muscle

The conventional analysis of the 2D-diffusion measurements demonstrated – as expected – clear differences between small metabolites, which diffuse faster, and lipid resonances (see Fig. 1). The results also show additional smaller differences between lipid resonances, which may lead to slightly varying lipid contributions in high DW spectra, depending on the diffusion weighting, or depending on the number of summed spectra from 2D measurements (see next paragraph).

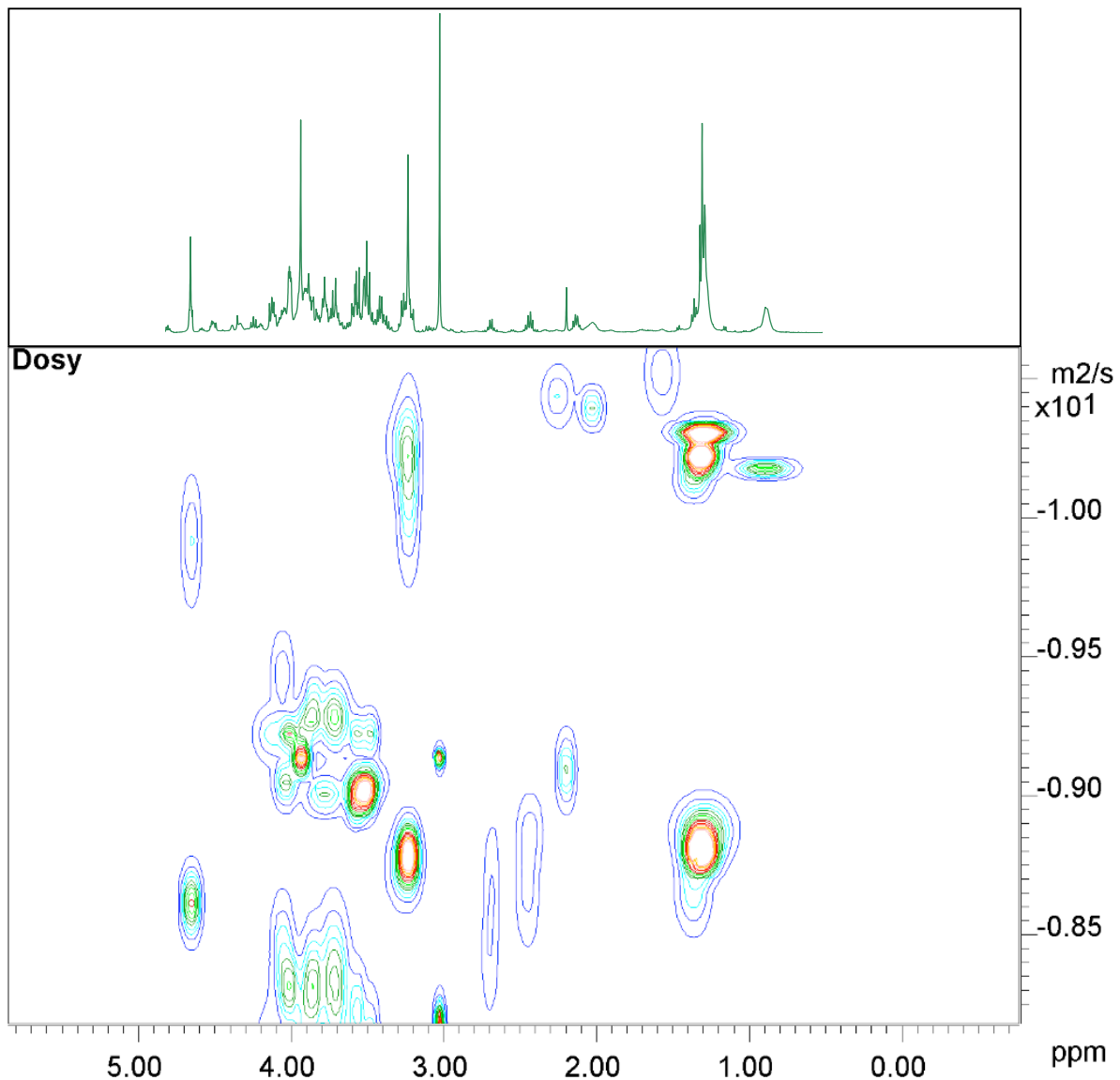


Figure 1: A 2D-DOSY plot of human muscle, with the corresponding 1D-CPMG spectrum shown above.

3.2 2D-Diffusion lipid removal

3.2.1 2D-diffusion for investigating diffusion properties and for "internal" lipid removal

The lipid removal procedure was first applied on human muscle using 2D-diffusion measurements by subtracting high-diffusion-weighted from low-diffusion-weighted spectra. Different numbers of spectra with strong and weak DW, respectively, were added from the pseudo 2D data, (1) to obtain sufficient SNR, (2) to determine and potentially adjust for slightly different spectral contributions of lipid moieties due to different diffusion constants. It turned out that the number of added spectra had only a minor influence on the spectral lipid contributions.

An example for the subtraction is shown in figure 2. The lipid spectrum subtraction removes the shoulder from the creatine peak at 3.0 ppm, and effectively suppresses the lipid broad component underneath the choline, taurine and glycerophosphocholine (GPC) peaks (Fig 2, insert). The strong overlap of the lactate peak at 1.3ppm or leucine, isoleucine and valine at $\sim 1.0\text{ppm}$ with lipids is similarly strongly reduced. The lipid peaks at 0.9 and 2.0ppm are well

suppressed, but small lipid residues remain, which are – besides residual artefacts – probably partly due to mobile lipids (19). Nevertheless, the residues still impede metabolite quantification or inclusion in chemometric methods. Therefore, for a chemometric analysis of small metabolites, the pure lipid regions (0.9 and 1.2ppm) need to be omitted. However, the procedure yields clearly reduced lipid contributions for several metabolites like lactate at 1.33ppm, choline, GPC, taurine, or creatine and may thus lead to more reliable metabolite estimations, while at the same time maintaining maximum signal strength without relaxation damping, which also hampers metabolite quantification. Furthermore, the pure lipid spectrum from the 2D diffusion data can be analyzed separately, besides the possibility to perform a regular diffusion analysis.

#	Lipid Part	ppm
1	ω -CH ₃	0.91
2	-(CH ₂) _n	1.3
3	β -CH ₂	1.59
4	-CH ₂ -CH=	2.03
5	α -CH ₂	2.26
6	=CH-CH ₂ -CH=	2.78
7	Tentatively assigned to CH ₂ lysyl protein	3.03
8	(-N ⁺ (CH ₃) ₃) Phosphatidylcholine)	3.25
9	CH ₂ -glyceryl	4.15
10	Cho- α -CH ₂ CH ₂ -glyceryl	4.35
11	-CH=CH-	5.32

Table 1: Lipid proton contributions for high DW spectra with their assigned chemical group structure and spectral position.

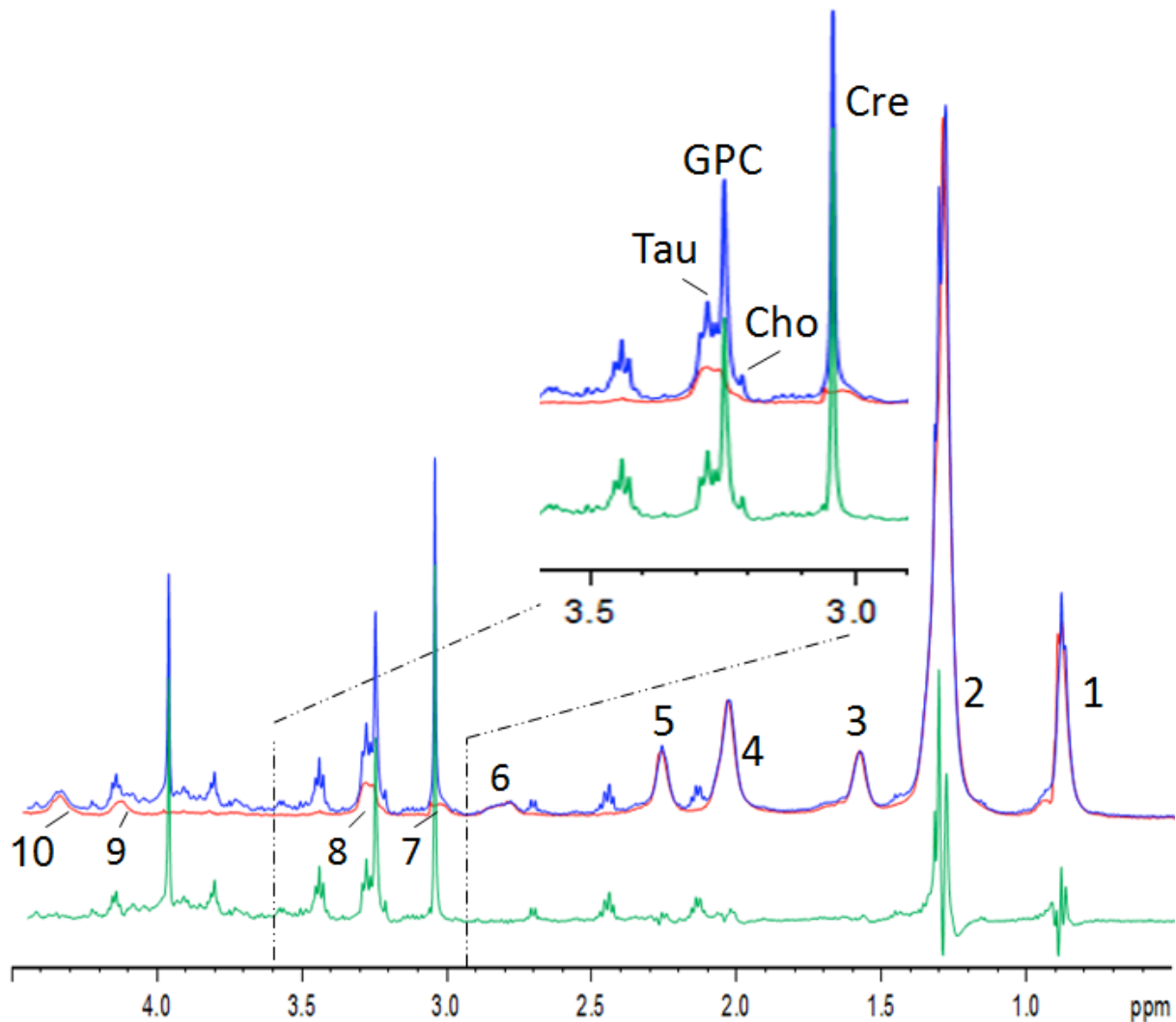


Figure 2: Example of human muscle diffusion spectra between 0.5 and 4.5ppm. Blue: summed spectrum with low DW showing small metabolite and strong lipid resonances; Red: summed spectrum with strong DW showing lipids only; Green: difference spectrum. Insert: zoomed region. Lipid resonances are assigned according to Table 1.

3.2.2 Removal of lipid contributions from CPMG spectra

1D CPMG spectra can be acquired fast with high SNR. Furthermore - as introduced earlier - lipid signals are reduced in CPMG spectra, because of shorter T₂ compared to small metabolites, though lower lipid contributions remain. The diffusion-based lipid removal method was therefore applied on standard CPMG spectra to determine if these remaining lipid contributions can be removed by subtracting the summed 20 high DW spectra of the 2D diffusion measurements from standard CPMG spectra. Thus, the effects of diffusion and relaxation differences were combined.

T₂ differences between lipid resonances (4) result in different signal intensities in CPMG spectra compared to those in standard 2D diffusion measurements. Therefore, a subtraction of the entire lipid spectrum after scaling with a single factor would leave remaining lipid signals, depending on their respective T₂ differences. Instead, a specific intensity scaling for each resonance in the high DW spectra was chosen to minimize the residue (but retaining frequency and line width). This procedure allows for an effective lipid removal (Fig. 3) and is similar to fitting the lipid resonances; however, without the problem to include resonances

from small metabolites into the fit. The figure demonstrates that the lipid contributions underlying some of the small metabolites are removed to a large extent. However, as for the subtraction of the high from the low DW spectra, residual artefacts remain at 0.9 and 1.2 ppm.

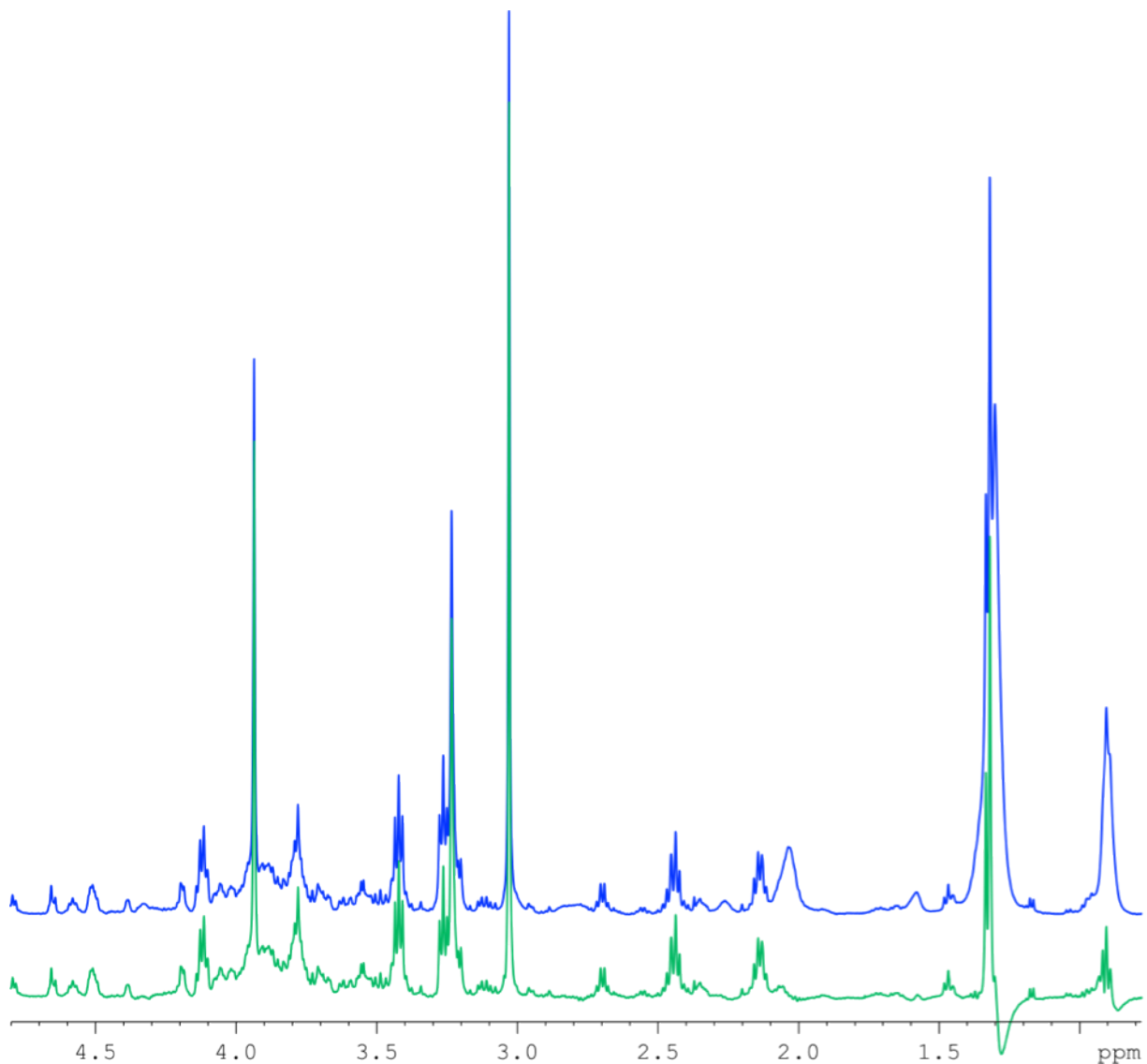


Figure 3: Example of human muscle spectra subtraction combining CPMG and diffusion spectra, using variable scaling of the lipid resonances. Blue: CPMG spectrum (512 transients). Green: Difference spectrum.

3.3 1D Diffusion-T2 filter Measurements for lipid removal

3.3.1 Echo Time variations – Parameter optimization

In a first step, the measurement parameters were optimized for the T2-filter part of our combined diffusion-CPMG sequence in order to find the best balance for the CPMG measurement between strong lipid reduction at longer echo times on one hand, and reduced SNR, potential sample heating and J-evolution on the other hand (4). Different echo times (TE) were tested for the original CPMG sequence, modifying the number of pulse loops and the interpulse delay time between 2 refocusing pulses for each loop (Table 2). Figure 4 shows a comparison between four CPMG spectra from one pork muscle biopsy acquired with different parameters according to Table 2.

Spectrum in Fig. 4	TE [ms]	Number of loops	Interpulse delay [ms]	Comment on spectra
1 – red	76.8	192	0.4	No visual J-modulation, good SNR
2 – green	152	380	0.4	No visual J-modulation, slightly decreased intensities, stronger decreased lipids
3 – cyan	152	38	4	Strong J-modulation
4 – blue	760	380	2	Lipids entirely suppressed, but J-modulation and strong reduction of metabolite intensities

Table 2: CPMG parameters applied for spectra shown in Fig. 4 (different TE, number of loops and interpulse delay time for each loop combination).

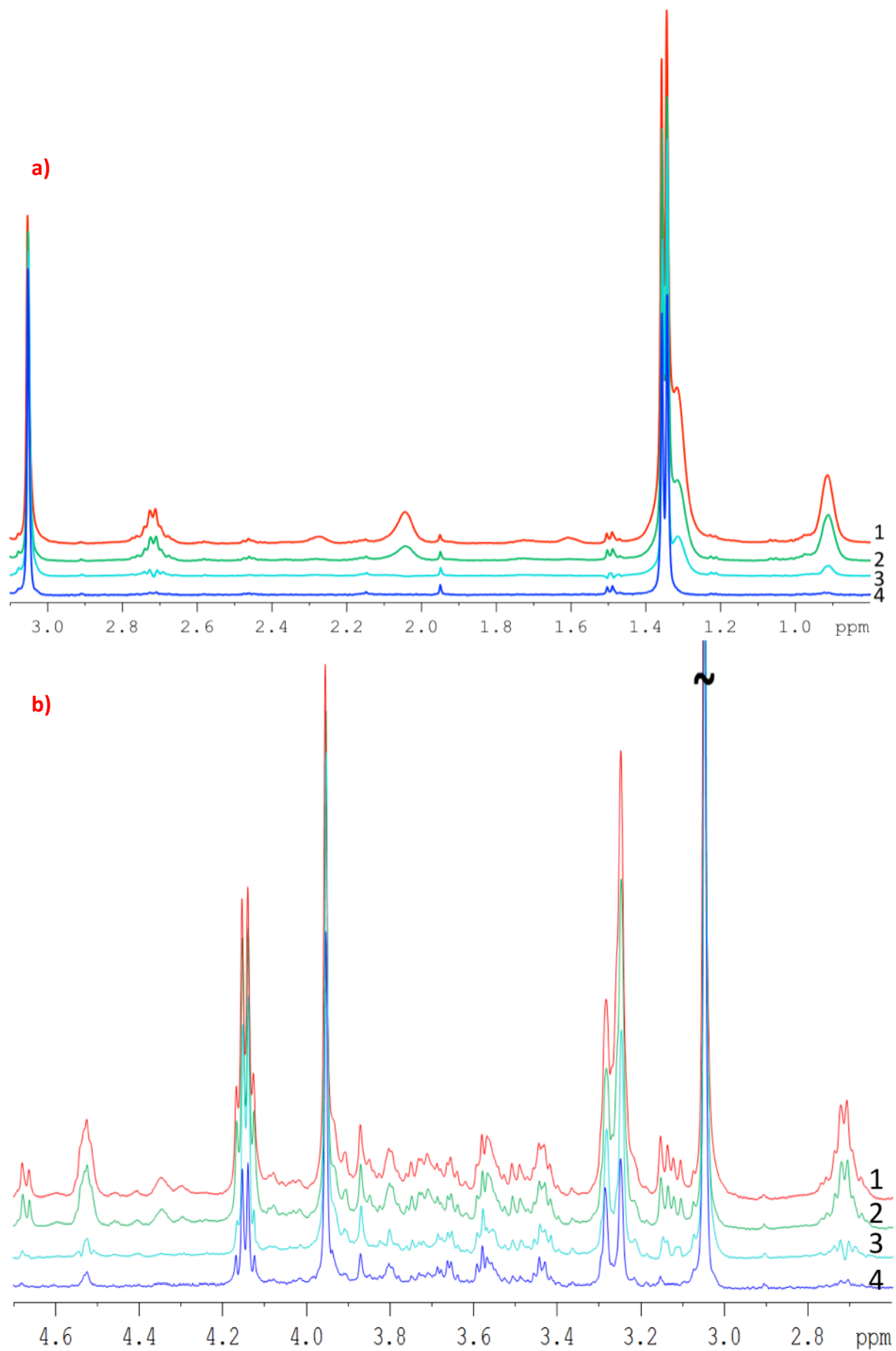


Figure 4: Example of pork muscle CPMG spectra acquired with different parameters (see table 2), all spectra are scaled to their creatine peak. a) Spectra between 0.8 and 3.1ppm. b) Spectra between 2.6 and 4.7ppm.

Spectrum 1 (TE=76.8ms) and spectrum 2 (TE=152ms) appear quite similar despite the doubled echo time, with only a small decrease of the peak intensity for the longer TE. Both spectra were acquired with 0.4ms interpulse delay time and do not demonstrate substantial J-modulation.

Spectrum 3 was acquired at the same TE as spectrum 2, but with a 10-times longer interpulse delay time (4ms). The strong J-evolution leads to complicated spectral patterns and reduced signal intensities (visually e.g. at 1.5, 2.7 or 3.15 ppm) hampering metabolite quantification and inclusion in metabonomic analysis. The much greater difference of spectrum 3 compared to spectra 1 and 2 points out the strong impact of the interpulse delay time for each loop (see also (24)).

Increasing the echo time to 760 ms reduced considerably the lipid content and yielded an almost fat free spectrum (spectrum 4). However, metabolite resonances were also clearly reduced at this long TE, as seen e.g. at the cysteine multiplet at 3.1ppm which disappears entirely in the noise, as well as clear intensity decreases of resonances between 3.5 and 3.8 ppm or at 2.7 ppm. Thus, increasing only TE appears not well suited for complete removal of lipid contributions, because of low SNR.

In conclusion, the results of the interpulse delay time and TE variation in the original CPMG sequence suggest that the combination of a CPMG sequence at moderate TE but short interpulse spacing with a DW module and subsequent lipid subtraction appears most promising for complete lipid removal while maintaining signals from small metabolites for analysis.

3.3.2 1D Diffusion-T2 filter lipid removal

The lipid spectrum subtraction method described in section 3.2 employed summed spectra with strong DW from a 2D diffusion measurement. Since the results showed that the number of added spectra had only low impact on spectral lipid contributions, a 1D-diffusion measurement would suffice for the lipid subtraction. The combination of this 1D-diffusion preparation with an optimized CPMG T2-filter in one sequence eliminated residual lipids from the muscle spectra, which were present in subtracted spectra without the T2 filter, thus permitting the separate analysis of a lipid free metabolite and a pure lipid spectrum (Fig. 5).

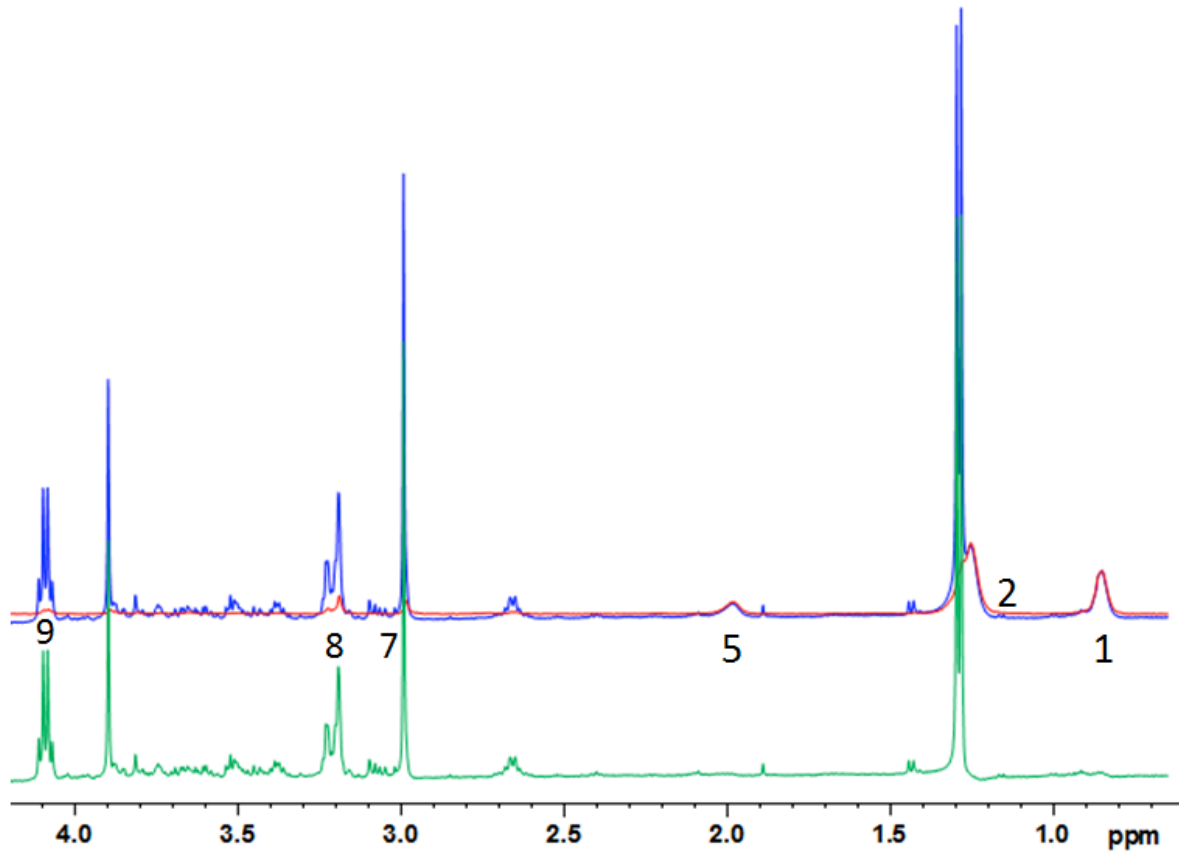


Figure 5: 1D Diffusion-CPMG spectra of a pork muscle (blue = low DW; red = strong DW; green = difference). For the lipid assignment, see Table 1.

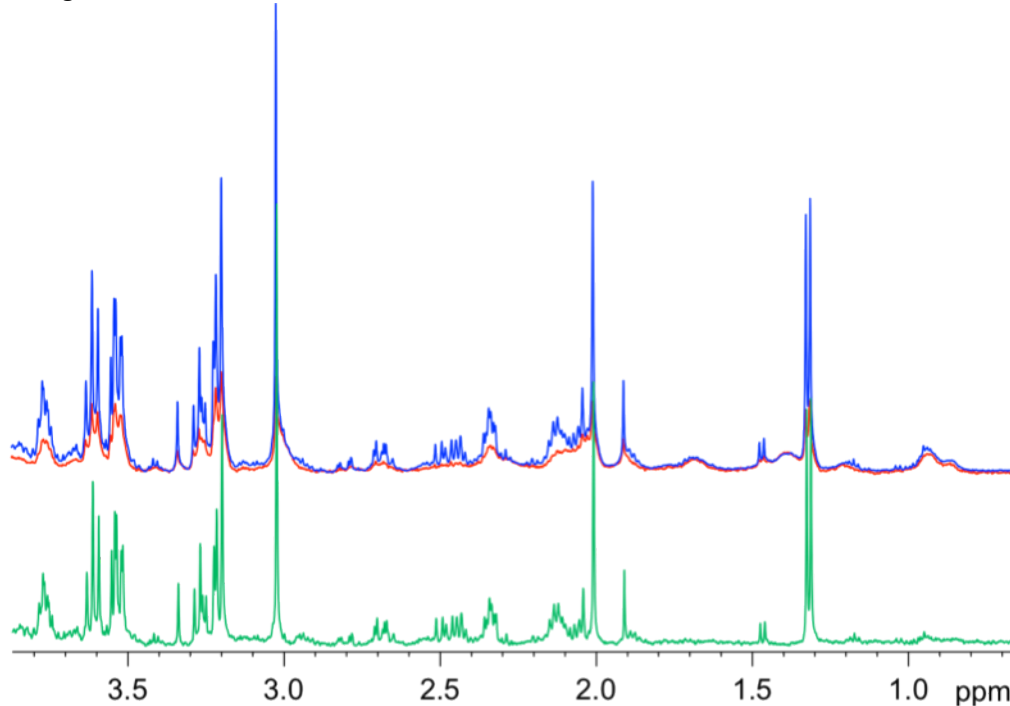


Figure 6: 1D Diffusion-CPMG spectra of a sheep brain (blue = low DW; red = strong DW; green = difference).

Similar results were obtained for spectra from sheep brain biopsies, though with much less prominent lipids (Fig.6) and in spectra of human liver with very strong lipid peaks (Fig.7); thus, suggesting that this method is applicable in various tissue types.

For the liver spectra, a residual lipid artefact can be seen at 1.2ppm after subtraction (Fig.7), probably due to the very high amount of lipid with the $-(CH_2)_n$ lipid peak being 20 times

higher than the creatine peak at 3.05ppm. However, the lactate peak is clearly detectable in the subtracted spectrum and appears unaffected from lipids (see insert). Lactate could thus be included in the metabonomic analysis, while it was almost hidden by lipids in the original spectrum (Fig.7 - insert).

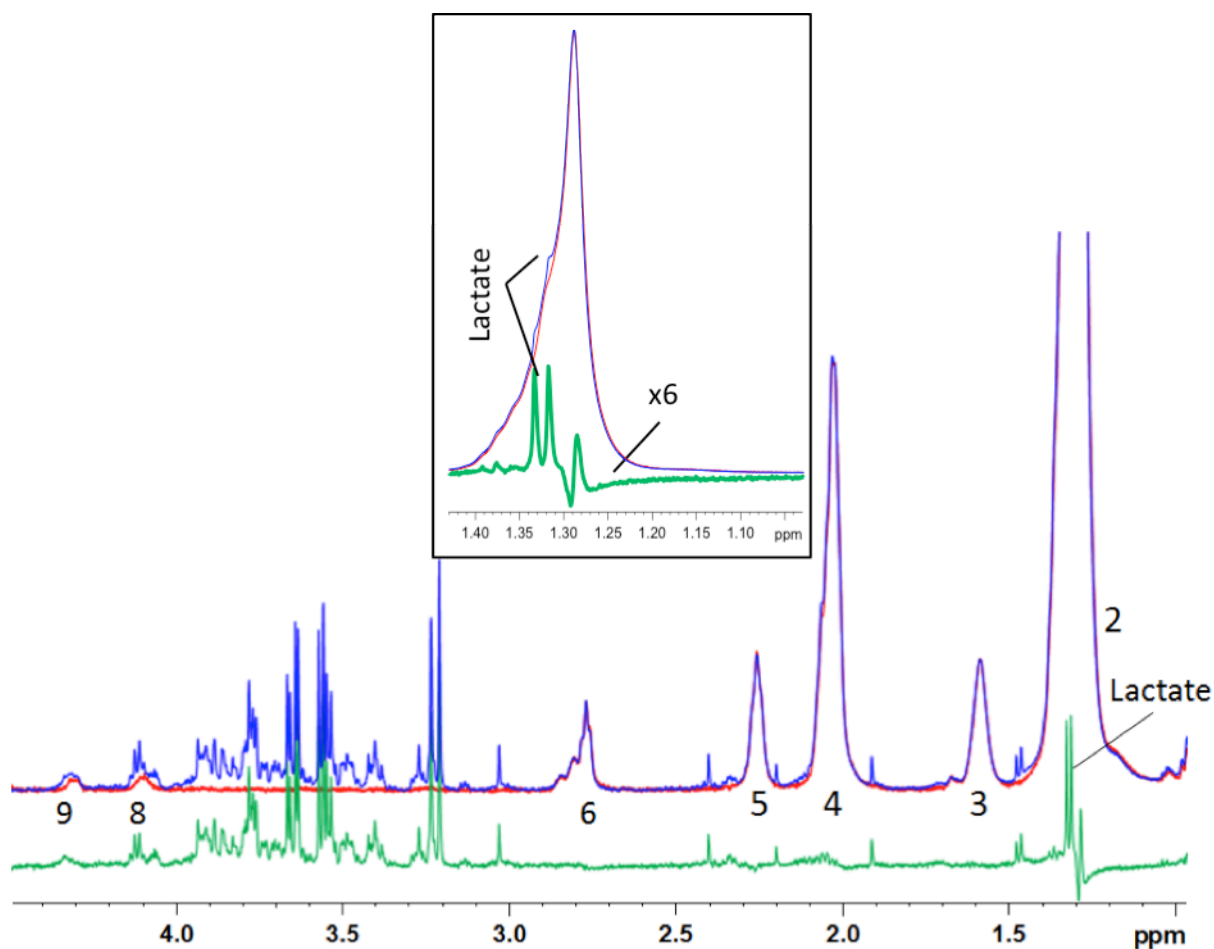


Figure 7: 1D Diffusion-CPMG spectra of a human liver sample (blue = low DW; red = strong DW; green = difference). For lipid assignment, see Table 1. Insert: Zoom on the 1.15-1.45 ppm region - The subtracted spectrum is increased 6 times for a better visualization of the lactate peak.

The 2D diffusion experiments permitted a flexible adjustment of strong and low diffusion weighted spectra for best balance between metabolite attenuation and SNR. However, after establishing the required DW for optimal lipid removal, 1D-diffusion measurements may be preferred in the future for better SNR and shorter scan times. The combined diffusion-CPMG sequence yielded high quality small metabolite and lipid spectra with no obvious spectral impairment compared to a regular CPMG sequence and benefits from amplification of simultaneous T2 and diffusion filters.

3.4 Same-Needle Biopsy Analysis: Comparison with and without diffusion spectroscopy editing

For testing the potential of the lipid removal procedure, original CPMG spectra of repeated measurements on same needle biopsies were analyzed and compared to the corresponding CPMG spectra with lipid subtraction, using the resonance-specific scaling, as described in 3.2.2.

Principal Component Analyses (PCA) of the entire spectrum (Fig.8) without lipid removal demonstrated clustering for most of the same needle biopsies, both on PC1/PC2 and PC2/PC3, indicating spectral similarities between them. However, because of considerable differences among same needle biopsies in few subjects there are no significant group differences for PC1 ($p=0.15$), PC2 ($p=0.23$) and PC3 ($p=0.05$).

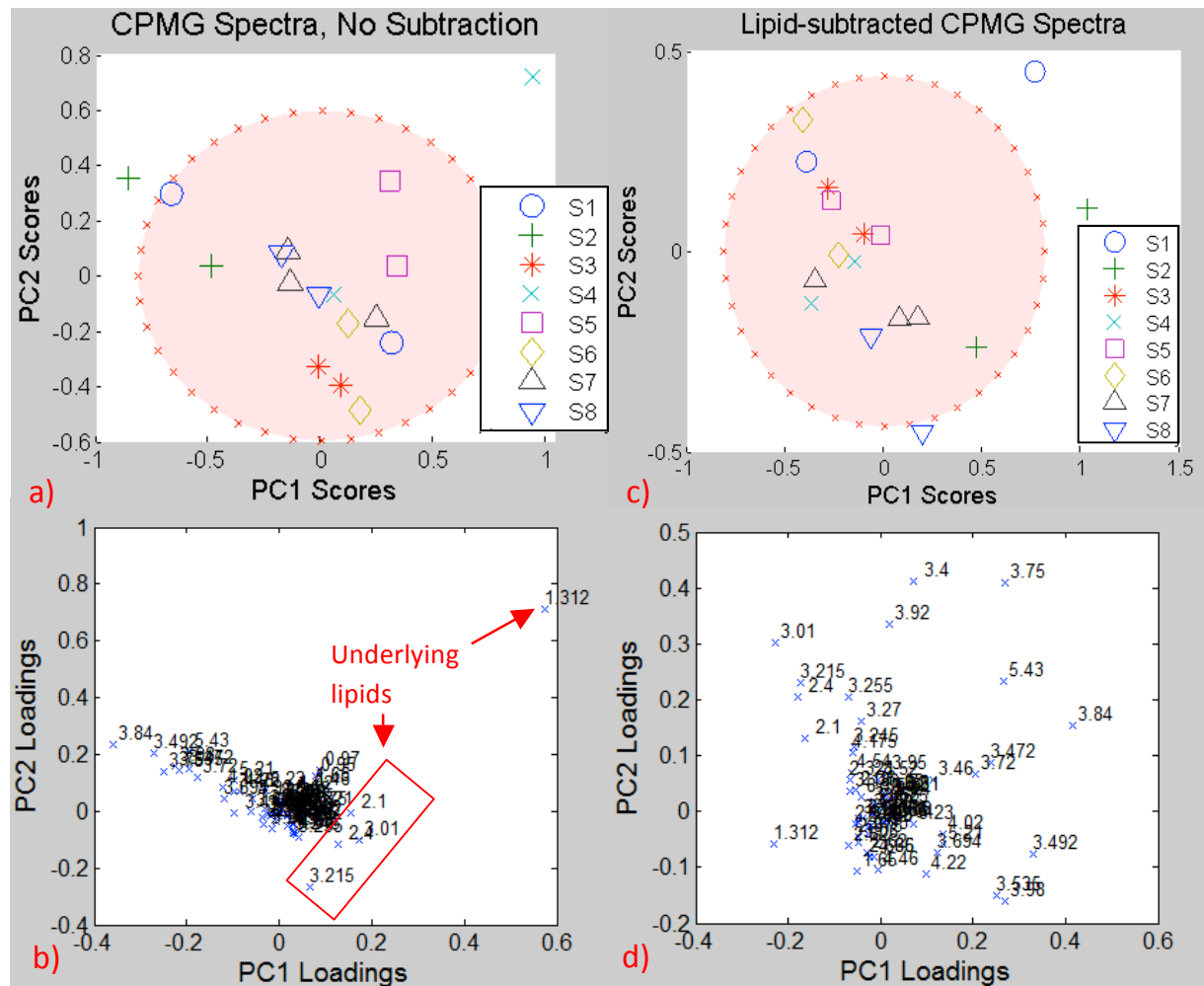


Figure 8: Same-needle biopsy analysis without lipid subtraction (left) and with lipid subtraction (right). Up : PCA, Down: Loading plots. Red ellipse: 95% confidence interval.

The PCA results reveal one biopsy (S4) outside of the 95% confidence interval (Fig.8a), and the loading plot (Fig.8b) indicates the bucket at 1.3 ppm as responsible for this separation, which is most likely due to the $-(CH_2)_n$ lipid group besides lactate. The loading plot from the PCA using non-subtracted spectra is dominated by lipid peaks (despite the exclusion of pure lipid regions from the analysis) and therefore reveals the possible influence of lipid content in chemometric analyses for metabolites that are biased by underlying lipid.

The analysis was repeated after lipid subtraction of the CPMG spectra in order to reduce the lipid contribution on the principal component analysis separation. The PCA from the lipid-removed spectra (Fig.8c) shows better clustering of same-needle biopsies (significant for PC2, $p=0.03$), as well as a more homogenous loading plot (Fig.8d). Thus, the PCA separation is due to a combination of different metabolites and not dominated by lipids as in the non-subtracted spectra. The two biopsies from sample S4 are much closer to each other after the lipid removal than before, indicating that the two biopsies have a similar metabolite but different lipid content. The results suggest that lipid removal in this reproducibility study

leads to clustering and group separation that is based predominantly on small metabolite differences instead of lipid contributions. If on the other hand lipid components are the focus of interest, the pure lipid spectra used for subtraction can be analysed accordingly in the absence of small metabolites.

A secondary aim of this reproducibility study was to investigate how far the metabolite profile of a single biopsy can be considered representative for the tissue under investigation. Same needle biopsies harvested from the same muscle demonstrated similarities but also quite surprisingly strong differences in the metabolites content as obtained from HR-MAS. This variability needs to be taken into account in longitudinal HR-MAS studies on muscle tissue but also for any other study that relies on the assumption that a biopsy sample represents a specific muscle type. It should be noted that the quite high variability also among same needle biopsies was not due to the spectral quality, but may be due to muscle fiber type composition (25). It has been suggested to use large biopsy samples to reduce intra-individual variation in the percentages of fast and slow fibers (26), although other studies have found only low variation in fiber type distribution within single biopsies (27). As discussed, a high variability in the lipid region may occur and is probably due to varying inclusions of small residual contributions from extramyocellular lipid despite careful prevention during biopsy harvesting.

4. Conclusion

Spectra of biopsies from many different organs show, besides small metabolites, strong contributions from lipids, which often even dominate the spectra. This strongly impedes correct small metabolite quantification and metabonomic analysis. To overcome this problem, we took advantage of diffusion differences between small metabolites and lipids combined with T2 differences to obtain lipid-free spectra.

A reproducibility study of same-needle muscle biopsy measurements demonstrated the applicability of the method and its potential value, by shifting the separation between groups from lipid contributions to different other metabolites. The elimination of lipids from the HR-MAS spectra and the resulting less biased assessment of small metabolites has thus potential to remove ambiguities in the interpretation of metabonomic results. Moreover, the diffusion scans permit a separate lipid analysis and a regular diffusion analysis without expanding measurement time.

Acknowledgement

This work was supported by the Swiss National Science Foundation SNF grant #320030-138150 (P.V.), SNF Ambizione grant PZ00P3_126339 (F.A.) and BASPO 11-09(F.A.).

Supplementary material

#	Reason for excluding the region
1	Lipid & Noise
2	Lipid

3	Lidocaine contamination
4	Lipid
5	Pure noise
6	Lipid
7	Lidocaine contamination & Lipid
8	Lipid
9	Lipid
10	Lidocaine contamination
11	Lipid
12	Water residue
13	Lipid
14	Pure noise
15	Pure noise
16	Lidocaine contamination & Noise
17	Pure noise

Table S1: Excluded regions from figure S1, with the reasons for exclusion

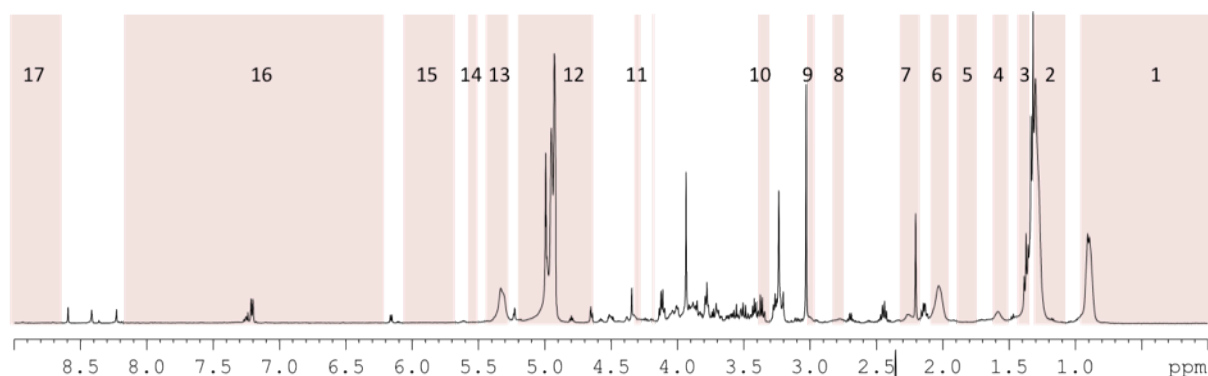


Figure S1: Muscle spectrum example, with the excluded regions in color, labelled according to Table S1.

Reference List

1. Lindon JC, Beckonert OP, Holmes E, Nicholson JK. High-resolution magic angle spinning NMR spectroscopy: Application to biomedical studies. *Progress in Nuclear Magnetic Resonance Spectroscopy* 2009; 55:79-100.
2. Graveron-Demilly D. Quantification in magnetic resonance spectroscopy based on semi-parametric approaches. *MAGMA* 2014; 27:113-130.
3. Righi V, Durante C, Cocchi M, et al. Discrimination of healthy and neoplastic human colon tissues by ex vivo HR-MAS NMR spectroscopy and chemometric analyses. *J Proteome Res* 2009; 8:1859-1869.
4. Rooney OM, Troke J, Nicholson JK, Griffin JL. High-resolution diffusion and relaxation-edited magic angle spinning ¹H NMR spectroscopy of intact liver tissue. *Magn Reson Med* 2003; 50:925-930.
5. Ribeiro JP, Palczewska M, Andre S, et al. Diffusion nuclear magnetic resonance spectroscopy detects substoichiometric concentrations of small molecules in protein samples. *Anal Biochem* 2010; 396:117-123.
6. Kaehlig H, Dietrich K, Dorner S. Analysis of Carbohydrate Mixtures by Diffusion Difference NMR Spectroscopy. *Monatshefte für Chemie* 2002; 133:589-598.
7. De Graaf RA, Behar KL. Quantitative ¹H NMR spectroscopy of blood plasma metabolites. *Anal Chem* 2003; 75:2100-2104.
8. Liu M, Nicholson JK, Lindon JC. High-resolution diffusion and relaxation edited one- and two-dimensional ¹H NMR spectroscopy of biological fluids. *Anal Chem* 1996; 68:3370-3376.
9. Kunz N, Cudalbu C, Mlynarik V, Huppi PS, Sizonenko SV, Gruetter R. Diffusion-weighted spectroscopy: a novel approach to determine macromolecule resonances in short-echo time ¹H-MRS. *Magn Reson Med* 2010; 64:939-946.
10. Chin JA, Chen A, Shapiro MJ. SPEEDY: spin-echo enhanced diffusion filtered spectroscopy. A new tool for high resolution MAS NMR. *J Comb Chem* 2000; 2:293-296.
11. Seland JG, S+©rland GH, Anthonsen HW, Krane J. Combining PFG and CPMG NMR measurements for separate characterization of oil and water simultaneously present in a heterogeneous system. *Appl Magn Reson* 2003; 24:41-53.
12. Vandusschoten D, deJager PA, VanAs H. Extracting Diffusion Constants from Echo-Time-Dependent PFG NMR Data Using Relaxation-Time Information. *Journal of Magnetic Resonance, Series A* 1995; 116:22-28.
13. Broskey NT, Greggio C, Boss A, et al. Skeletal muscle mitochondria in the elderly: effects of physical fitness and exercise training. *J Clin Endocrinol Metab* 2014; 99:1852-1861.
14. Amati F, Dube JJ, Alvarez-Carnero E, et al. Skeletal muscle triglycerides, diacylglycerols, and ceramides in insulin resistance: another paradox in endurance-trained athletes? *Diabetes* 2011; 60:2588-2597.
15. Oostendorp M, Engelke UF, Willemsen MA, Wevers RA. Diagnosing inborn errors of lipid metabolism with proton nuclear magnetic resonance spectroscopy. *Clin Chem* 2006; 52:1395-1405.

16. Sharma U, Atri S, Sharma MC, Sarkar C, Jagannathan NR. Biochemical characterization of muscle tissue of limb girdle muscular dystrophy: an ^1H and ^{13}C NMR study. *NMR Biomed* 2003; 16:213-223.
17. Righi V, Andronesi O, Mintzopoulos D, Tzika AA. Molecular characterization and quantification using state of the art solid-state adiabatic TOBSY NMR in burn trauma. *Int J Mol Med* 2009; 24:749-757.
18. Srivastava NK, Pradhan S, Mittal B, Kumar R, Pandey CM, Gowda GA. Novel corrective equations for complete estimation of human tissue lipids after their partial destruction by perchloric acid pre-treatment: high-resolution (^1H) -NMR-based study. *NMR Biomed* 2008; 21:89-100.
19. Zietkowski D, Davidson RL, Eykyn TR, De Silva SS, Desouza NM, Payne GS. Detection of cancer in cervical tissue biopsies using mobile lipid resonances measured with diffusion-weighted (^1H) magnetic resonance spectroscopy. *NMR Biomed* 2010; 23:382-390.
20. Hakumaki JM, Kauppinen RA. ^1H NMR visible lipids in the life and death of cells. *Trends Biochem Sci* 2000; 25:357-362.
21. Liu M, Tang H, Nicholson JK, Lindon JC. Use of ^1H NMR-determined diffusion coefficients to characterize lipoprotein fractions in human blood plasma. *Magn Reson Chem* 2002; 40:S83-S88.
22. Dieterle F, Ross A, Schlotterbeck G, Senn H. Probabilistic quotient normalization as robust method to account for dilution of complex biological mixtures. Application in ^1H NMR metabolomics. *Anal Chem* 2006; 78:4281-4290.
23. Wiklund S. Multivariate data analysis and modeling in "omics". *Umetrics* 2008.
24. Beckonert O, Coen M, Keun HC, et al. High-resolution magic-angle-spinning NMR spectroscopy for metabolic profiling of intact tissues. *Nat Protoc* 2010; 5:1019-1032.
25. Vermathen P, Kreis R, Boesch C. Distribution of intramyocellular lipids in human calf muscles as determined by MR spectroscopic imaging. *Magn Reson Med* 2004; 51:253-262.
26. Staron RS, Hagerman FC, Hikida RS, et al. Fiber type composition of the vastus lateralis muscle of young men and women. *J Histochem Cytochem* 2000; 48:623-629.
27. Blomstrand E, Ekblom B. The needle biopsy technique for fibre type determination in human skeletal muscle--a methodological study. *Acta Physiol Scand* 1982; 116:437-442.